Morphology of the implantation-induced disorder in GaAs studied by Raman spectroscopy and ion channeling

U. V. Desnica, I. D. Desnica-Franković, M. Ivanda, and K. Furić
R. Bošković Institute, P.O. Box 1016, Zagreb, Croatia

T. E. Haynes
Oak Ridge National Laboratory, Oak Ridge, Tennessee 37831
(Received 29 October 1996; revised manuscript received 6 February 1997)

Disorder was introduced into GaAs by implantation of $^{30}Si^{+}$ ions, using a very wide range of ion doses, dose rates, and implant temperatures, and studied by Raman scattering (RS) and Rutherford backscattering ion channeling (RBS). RS spectra were deconvoluted consistently and systematically into up to four components, one of them being an apparent background signal interpreted here as a boson peak. Arguments are given that this signal represents the second amorphous phase different from a continuous random network. An intercascade distance model (ICD) was postulated, which estimates the average distance, L_{ICD}, between implantation-induced cascades as a function of ion dose. An analogous parameter, L_{RBS}, was calculated from the RBS damage fraction f_{RBS}. From RS data the correlation length L_{RS}, representing the size of crystalline regions with preserved translational symmetry, was determined by fitting the LO signal within the spatial correlation model. All three L's agree nicely, proving the equivalency of the correlation length and intercascade distance. This enabled a straightforward comparison of relevant signals and a direct correlation between RS and RBS. While measure of damage in RBS (f_{RBS}) reflects the disordered volume fraction of the implanted layer, RS measures simultaneously the lowering of the translational symmetry (an effect that prevails at lower doses) and the fraction of disordered volume (prevailing at higher doses). A considerable difference in sensitivity between RS and RBS to particular defects enabled the differentiation of six different types of implantation-introduced disorder. [S0163-1829(97)06524-7]

I. INTRODUCTION

Disordered (particularly amorphous) semiconductors have attracted considerable interest due to a number of theoretically intriguing aspects and also due to their important role in many current and future technologies.[1] While in perfect crystalline semiconductors characteristic properties are generally well defined, in disordered semiconductors most properties (optical, electrical, vibrational, structural, thermodynamic, etc.) depend on the preparation conditions and/or thermal history.[2] Traditionally, tetrahedrally coordinated amorphous semiconductors have been envisioned as a continuous random network (a-CRN) of host atoms, which was assumed to be the only amorphous phase.[3–7] However, based on the reinterpretation of the observed background signal in Raman spectra, it has been proposed that in a-Si (Ref. 8) and a-GaAs (Refs. 9 and 10) an additional amorphous structure exists, which has a specific medium-range order (MRO). This peculiar structure, common in glassy materials, causes an excess in the vibrational density of states (in comparison to the expected Debye value), resulting in a broad band, the so-called ''boson peak'' (BP) in Raman spectra.[9–11] Up to now, the MRO structure has not been directly visualized (by high-resolution transmission electron microscopy or atomic force microscopy) in either glasses or in vitreous amorphous semiconductors but is manifest in spectra of inelastic neutron scattering, x-ray diffraction, infrared absorption, low-temperature excess specific heat and thermal conductivity plateaus,[12–14] and Raman scattering.[15] Hence the microscopic origin of these ''excess'' vibrational states causing ''boson peak'' remains controversial.[16–20] Several, usually material-specific, models were proposed, such as the involvement of ''soft'' anharmonic potentials,[17] dipolar interactions between defects,[18] the involvement of clusters or structural correlations,[19] and the existence of MRO structures with fractionlike dynamics above a certain frequency.[20] In this paper we have adopted this last approach, since there are sound arguments that it is the most appropriate[9,21] and since presented experimental results are consistent with such an interpretation, giving it new support. As in glassy solids, MRO was not hitherto directly seen in tetrahedral semiconductors, but there are indications that it is present in this class of materials as well.[9,21,22] However, this particular choice of interpretation of the ''background'' part of the RS spectra is not critical for this paper, the main point being the observation that the apparent ''background'' is in fact a meaningful signal, equivalent to the analogous signal in glassy solids (BP), regardless of which exact microscopic structure gives rise to this signal. Such an interpretation of BP in a-GaAs establishes an exciting common link between tetrahedral semiconductors and otherwise very different glassy materials.

Implantation-induced disorder is of particular scientific interest in this regard so that issues such as noncrystallinity and the possible existence of an atomic-scale structure(s) intermediate to that of the crystalline and amorphous forms can be probed.[3] When partly disordered by implantation, GaAs becomes effectively a semiconductor nanocomposite (in analogy with nanocomposites in sol-gel ceramics,[23] i.e., a composite of amorphous GaAs and GaAs nanocrystals or

 © 1997 The American Physical Society

microcrystals). Thus ion implantation allows the incremental introduction of disorder and can enable fundamental studies of the creation and dynamics of disorder, from defect nucleation until (and even after) the amorphous state is reached. Furthermore, various factors influencing morphology and the amount of disorder can be studied by changing external parameters of the implantation. In this work, ion implantation is used in this way and for that purpose.

Both Raman spectroscopy (RS) and Rutherford backscattering (RBS) ion channeling have been used extensively to monitor overall changes in microstructure of implanted samples. However, an analysis that would enable a direct comparison of ''figures of merit,'' i.e., changes in characteristic signals that would be appropriate for the disorder assessment in each method, is still lacking. An attempt in that direction has shown that such a comparison might be helpful in differentiating some disordered structures.[24,25] For a meaningful comparison of the two methods, it must be proven that they have equivalent definitions of some basic disorder properties, such as ''amorphous,'' ''crystalline,'' etc. It is not always the case, and there are many known examples where different characterization techniques may saturate, and thereby imply amorphization, at quite different doses.[26] It will be shown in this paper that RS and RBS results could be directly compared since both techniques indicate that amorphization occurs at the same dose [both crystalline components (LO and TO) in RS spectra vanish at the same dose at which the RBS damage refraction reaches unity (Fig. 3)]. Furthermore, it will be shown in Sec. IV B that both RS and RBS give similar values for the correlation length L, which measures the size of undamaged crystal regions.

In this paper, results of Raman and ion channeling studies of the disorder and its morphology in Si implanted GaAs are presented. A very large range of Si ion doses, ion dose rates, and substrate temperatures has been applied. The aim of this paper is twofold: first, to identify and analyze various mechanisms that are responsible for different sensitivities of RS and RBS to various types of disorder (Sec. IV A). We have analyzed possible mechanisms influencing RBS and Raman signals, and proposed a physical picture that enables meaningful qualitative and even quantitative comparison between these two methods, and predicts for which types of disorder either particular method should be more sensitive. Second, we apply these findings to analyze GaAs layers disordered in a controlled way by ion implantation, by changing the ion dose (Sec. IV B), ion dose rate (Sec. IV C), and substrate temperature (Sec. IV D). It is demonstrated that at least six different components of the damage can be successfully separated, which yields better understanding of the disorder and disorder morphology evolution during ion implantation in GaAs.

II. EXPERIMENTAL TECHNIQUES

The starting material was liquid encapsulated Czochralski (LEC) grown, undoped, semi-insulating, (100)-oriented GaAs, with a dislocation density in the $10^4/\mathrm{cm}^2$ range. $^{30}\mathrm{Si}^+$ was implanted at an energy of 100 keV into substrates tilted 7° with respect to the incident beam to minimize channeling effects. Precautions were taken to control the implantation temperature, as described previously.[27,28] Six series of samples were implanted: (a) different ion doses in the range $8\times10^{12}/\mathrm{cm}^2-3\times10^{15}/\mathrm{cm}^2$ at low dose rate (0.05 $\mu\mathrm{A/cm}^2$); (b) ion doses in the range $1\times10^{15}/\mathrm{cm}^2-3\times10^{16}/\mathrm{cm}^2$ at high dose rate (1.0 $\mu\mathrm{A/cm}^2$); (c) different dose rates at a fixed ion dose $2\times10^{14}/\mathrm{cm}^2$; and (d)–(f) three series of samples for which three selected doses (and the same low dose rate) were kept constant but substrate temperature was varied in the -190 °C to $+40$ °C range.

First-order, dipole-allowed Raman spectra were obtained at room temperature (RT) by excitation with the 2.57-eV (514.5-nm) line from an Ar-ion laser, with low laser power (0.4 W) to avoid heating. The probing depth for both crystalline and amorphous GaAs regions is shallower than the thickness of the implanted layer, which is approximately 100 nm, so that the undamaged underlying substrate does not contribute to the Raman spectra. The scattered light was filtered with a triple spectrometer (DILOR Z-24) and Raman spectra were taken in the 190–320-cm^{-1} range, with 1-cm^{-1} step. This or a similarly limited frequency range is often used in Raman analysis[3–5,29,30] since in this range all RS signals characteristic of implanted GaAs can be observed, including two crystalline modes [longitudinal optical LO(Γ) peak at 290 cm^{-1} and transversal optical TO(Γ) at 268 cm^{-1}], the most prominent amorphous band (centered at 250 cm^{-1}), and also a part of the very broad BP. This peak has a maximum below 100 cm^{-1}, and decreases slowly and monotonously up to about 1000 cm^{-1}, so that in a small frequency range 190–320 cm^{-1} its intensity is well approximated as a linear function of frequency.

For ion channeling (RBS), backscattered ions from a 2-MeV He^+ beam were detected at a scattering angle of 160°. The probing beam was aligned with the $\langle100\rangle$ axis of the crystal. Damage profiles were extracted from the RBS spectra by subtracting the dechanneling portion of the yield, and correcting for the dechanneled fraction of the beam as a function of depth.[31] RBS damage fraction (f_{RBS}) is defined as the volume fraction of all atoms in the ion-implanted layer, which are disordered by implantation. All RBS and RS measurements were done at RT several months after implantation. This ensured complete stabilization of implant disorder, since part of the damage is known to anneal at RT over time scales of the order of days or even weeks.[28,32]

III. RESULTS

Examples of first-order Raman and RBS spectra depicting ion dose effects on representative samples from series (a) and (b) are presented in Figs. 1 and 2, respectively. In the unimplanted sample [Fig. 1(A)], a sharp LO(Γ) line at 290 cm^{-1} is absolutely dominant. Note especially that the TO peak at 268 cm^{-1} is absent, since it arises from a symmetry-forbidden scattering in the (100)-oriented zinc-blende structure. With increasing dose other contributions become important, particularly the TO peak at 268 cm^{-1}, and a band at 250 cm^{-1}, which is generally accepted to originate from the continuous-random-network structure of the amorphous phase (a-CRN).[3,33] The BP signal also continuously increases with the dose. At doses around $3\times10^{15}/\mathrm{cm}^2$ (CA dose) both crystal-related peaks practically disappear, indicating complete amorphization of the layer. Similarly, in

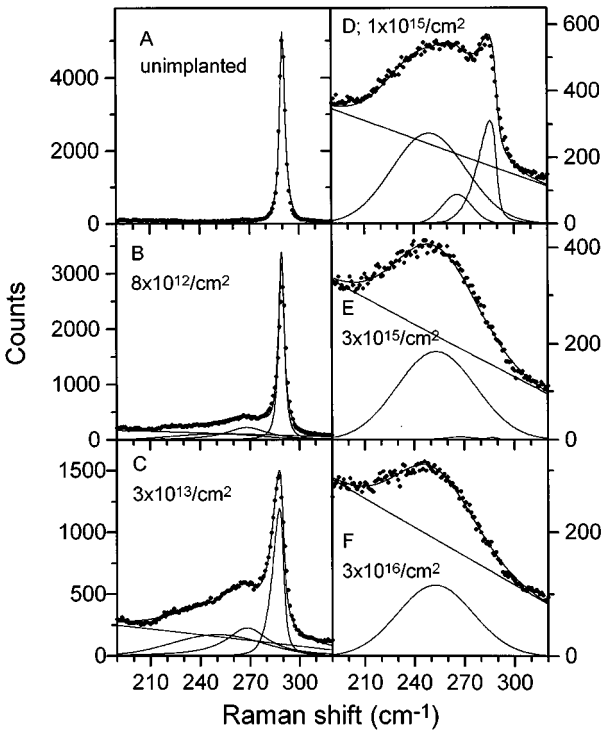

FIG. 1. Raman spectra of 100-keV $^{30}Si^{+}$-implanted GaAs, obtained using 2.41-eV excitation line polarized along the (110) direction, without polarization determination for the scattered light. Implantation doses are indicated in the figure, the implant current density was 50 nA/cm^2 for (B)–(E), and 1000 nA/cm^2 for (F). (A) represents Raman spectrum for unimplanted sample. Decomposition of spectra and fitting procedure are explained in the text.

RBS spectra the total damage increases up to dose 3×10^{15}/cm^2, where it reaches the same backscattered yield as from the random direction. Further implantation just slightly increases the thickness of the amorphized layer.

The kinetics of the accumulation of implantation-induced disorder as a function of ion dose is presented in Fig. 3.

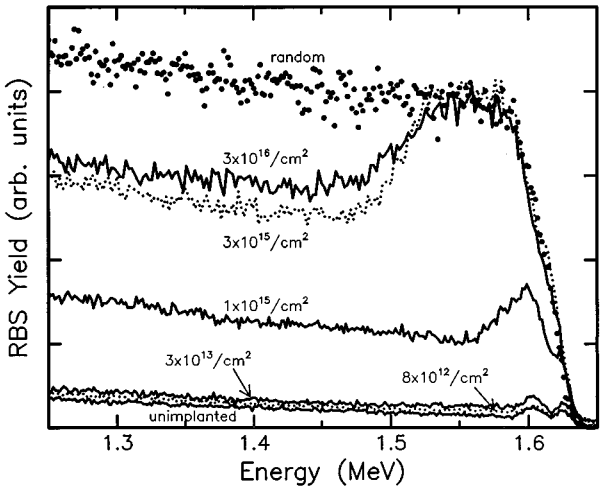

FIG. 2. Ion channeling spectra for 2.0-MeV ^{4}He ions scattered at 160° from GaAs samples after implantation with ^{30}Si ions at the indicated doses. The channeling direction was along a ⟨100⟩ axis.

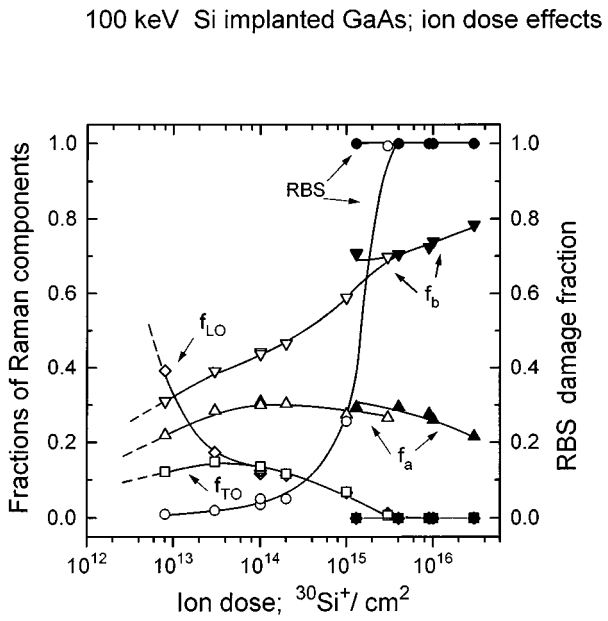

FIG. 3. Ion dose dependence of fractions of Raman components as determined from fitting and decomposition of RS spectra (left y axis) and the fraction of displaced atoms in the implanted layer, as determined with RBS (right y axis). Open symbols refer to the dose rate of 0.05 μA/cm^2, and solid symbols to the dose rate of 1 μA/cm^2. Lines are added to guide the eye.

Raman fractions are defined as relative intensity ratios of the particular peak to the total Raman signal. As expected, the Raman fraction of the LO peak ($f_{\mathrm{LO}}=I_{\mathrm{LO}}/I_{\mathrm{tot}}$), representing the monocrystalline, undamaged portion of the layer, decreases monotonously with the dose. The TO fraction f_{TO} indicates the presence of misoriented crystallites, i.e., some portion of the layer that was highly disordered during implantation and then randomly recrystallized. This polycrystalline component first increases with dose, and then decreases down to a total disappearance. It is interesting and important that only the BP fraction f_b continues increasing with dose over the entire range of doses. It is particularly interesting also that f_a (a-CRN fraction) first increases, then saturates, and finally starts to decrease with dose. This trend of the increase of f_b at the expense of f_a continues even after complete amorphization of the layer. Although these Raman fractions do not represent absolute volume fractions of each component they clearly show trends in accumulation of particular types of damage with dose, and indicate the presence of each fraction at the particular dose, as well as possible transformations of one fraction into the other. RBS results, presented in the same figure, show that most of the implanted volume is damaged within last order of magnitude below the CA dose. For doses higher than the CA dose (when $f_{\mathrm{RBS}}=1$), RBS cannot distinguish changes in the morphology of the disorder resulting from additional implantation.

The process of amorphization with implantation is usually analyzed through the ratio of intensities of crystalline and amorphous component-related signals in RS.[24,34] Now that we have indication of a second amorphous phase, we have analyzed them separately, with I_a denoting the integral of the a-CRN peak, and I_b denoting the integral of the BP component. Figure 4 shows a monotonic decrease of I_{LO}/I_a with

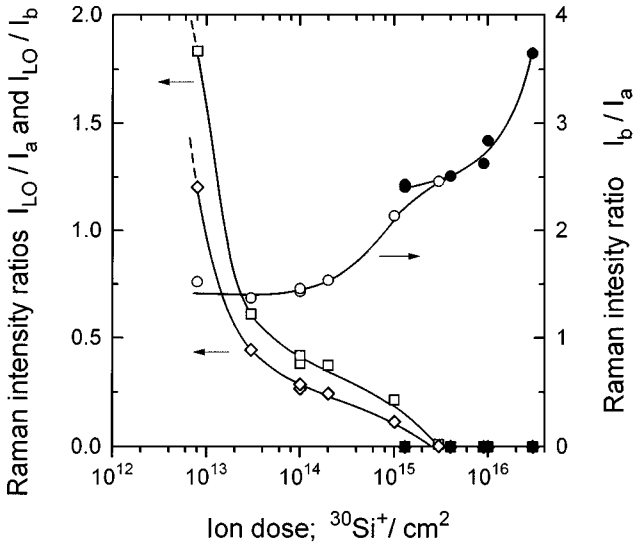

FIG. 4. Ion dose dependence of Raman intensity ratios of LO crystalline to amorphous components (left *y* axis), and intensity ratio of boson to random amorphous components (right *y* axis). Lines are added to guide the eye.

dose (I_{LO} denotes the integral of the LO peak). The I_{LO}/I_b ratio shows essentially the same trend, and both simply track the conversion of the GaAs crystal to amorphous GaAs. The I_b/I_a ratio remains practically constant for lower doses, and increases continuously for higher doses, indicating a significant change in the morphology of the amorphous part. This morphology change begins even before RBS detects complete amorphization, and moreover continues thereafter.

The same ratios are presented in Fig. 5 for series (c), where the samples were all implanted with the same dose but with different ion dose rates. The RBS damage signal increases drastically with ion dose rate (from less than 10% for low rates to over 80% for highest rate). However, the RS ratios I_{LO}/I_a and I_{LO}/I_b decrease only slightly with rate. Similarly, the I_b/I_a increases only slightly with rate.

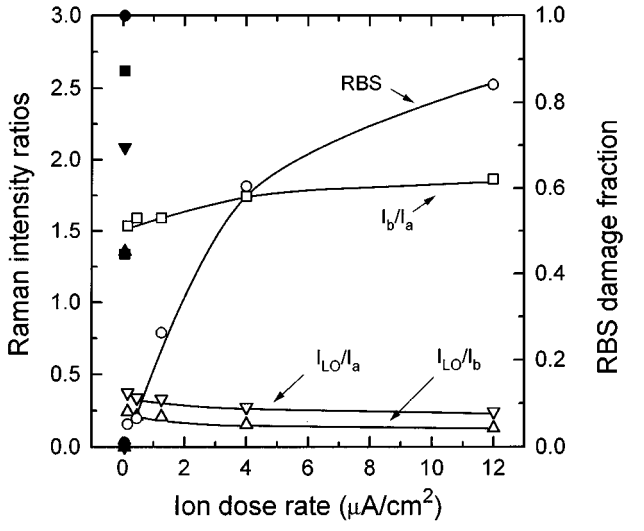

FIG. 5. Dose rate dependence (open symbols) of Raman intensity ratios (LO crystalline to amorphous components and boson to random amorphous components; left *y* axis), and fraction of displaced atoms in implanted layer, as determined with RBS (right *y* axis). Lines are added to guide the eye. The range of each ratio for all applied doses is also shown (for the rate 0.05 μA/cm^2; solid symbols).

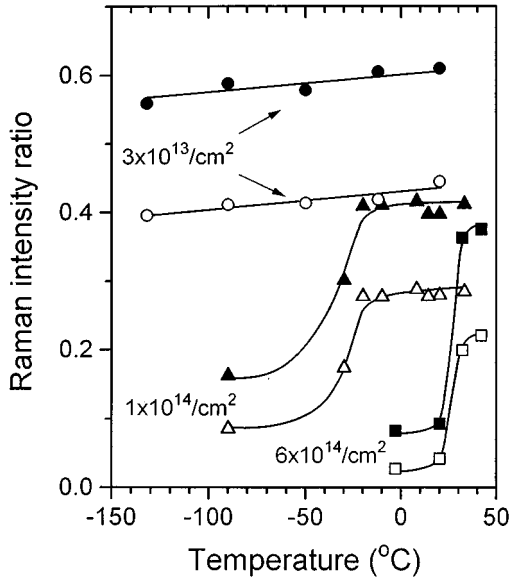

FIG. 6. Raman intensity ratios (crystalline to amorphous components) as a function of implant temperature, for three different doses. Open symbols depict I_{LO}/I_b ratio, while solid symbols depict I_{LO}/I_a ratio. Lines are added to guide the eye.

Finally, the effect of substrate temperature on the disorder is presented in Figs. 6 and 7, for three series of samples, each series implanted with a single ion dose (3×10^{13}/cm^2, 1×10^{14}/cm^2, or 6×10^{14}/cm^2, respectively) at a low dose rate

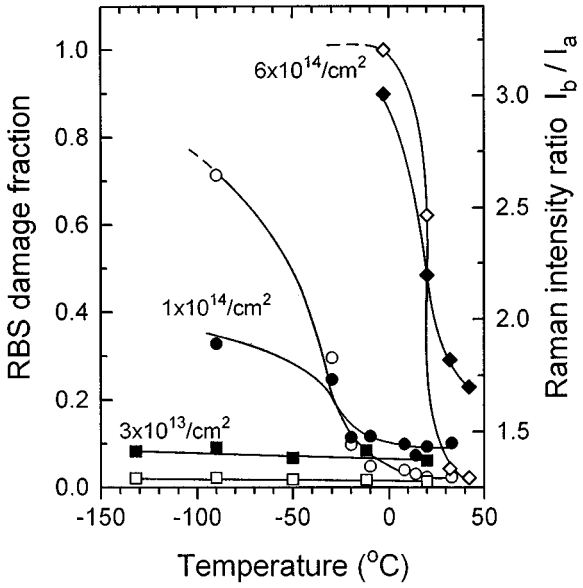

FIG. 7. RBS detected fraction of displaced atoms (left axis, open symbols) and Raman intensity ratio (boson to random amorphous components; right axis, solid symbols) as a function of implant temperature, for three different doses. Lines are added to guide the eye.

($0.05\ \mu A/cm^2$). At the lowest dose both I_{LO}/I_a and I_{LO}/I_b are large and practically constant, due to the absence of significant amorphization. On the other hand, at two higher doses, both ratios increase with implant temperature until they reach approximately a constant value. The difference between these two doses is that for the higher dose the constant value is lower for both components and it is reached only at a higher implant temperature (Fig. 6). The temperature range where the changes of ratios occur corresponds to the range of the most dramatic decrease of RBS detected damage. This is valid for both doses.

IV. DISCUSSION

A. Comparison of RS and RBS detection of disorder

RBS detects atoms that are displaced from their crystal-lattice sites. This makes it sensitive (though with some variations in sensitivity) to all types of disorder that involve such displacements. Hence RBS is a quantitative method but nonspecific to defect type. RS spectroscopy, on the other hand, can provide defect-specific information, but is generally not as quantitative. Hence they may give complementary information. However, in the various experiments described above, either one or the other method seems much more sensitive, which might be confusing. On the other hand, if different sensitivities for different types of defects are well understood, the comparison can be used to differentiate those defects. For example, there are dramatic changes in Raman signals for very low doses,[34] where the RBS signal is still nonexistent or is very small (Fig. 3). Similarly at high implant temperatures, the RBS signal drops practically to zero,[35] while the Raman ratios indicate that a considerable amount of damage is still present in the crystal, including some amorphization (Figs. 6 and 7). On the other hand, in some cases sensitivity to the disorder seems considerably higher for RBS than for RS (Fig. 5), particularly the increase of the disorder with dose rate.

In RBS the maximum signal is obtained for complete amorphization of the implanted crystal ($f_{RBS}=1$). The lower limit of the method is determined by the background scattering yield (primarily scattering from the surface atoms), which is typically 2–3% of the maximum signal. Hence, the range of sensitivity of RBS covers doses approximately two orders of magnitude below CA dose. In principle, f_{RBS} should correspond and be proportional to the total volume fraction of the layer, which is disordered with implantation (all types of disorder included). However, some particular types of disorder, such as small volume defects, for example, clusters of point defects (interstitials), can block the entire open channel between two adjacent rows of crystal atoms, thereby effectively contributing to the RBS signal much more than they should according to their actual volume fraction of the layer.[24] Still, in order to be observed by RBS at all, the concentration of these small-volume defects has to be quite large, of the order of 1% or so.

In RS the increase of disorder results in both the decrease of signal from undamaged monocrystalline fraction and the increase of signals characteristic of different types of disorder. Hence, the ratio of the sum of intensities of different disorder-related signals I_d (when properly weighted with specific scattering cross sections) to I_{LO} should be proportional to the disordered volume fraction. However, there are some specific types of disorder or defects, which will strongly affect Raman spectra even in cases when the volume fraction of these defects is very small, i.e., $f_{RBS}\cong 0$. Namely, stringent symmetry-related selection rules and the momentum conservation rule $\mathbf{q}=0$ are strictly satisfied only in a perfect crystal. However, in a damaged crystal the translation symmetry along the crystal is no longer preserved due to the loss of long-range order. The conservation rule then spans a certain range of wave numbers of order $1/L$, where L is the correlation (phonon localization) length, i.e., an average size of the undamaged region. Relaxation of conservation rules leads to the progressive attenuation of the LO peak intensity [Eq. (1) in Ref. 6, also Refs. 5, 36, and 37]. If the crystal is, for example, portioned by some line defects, this effect will be strong even for a relatively small total number of atoms involved in these line defects. (It is easy to estimate that, for example, a line defect density that would involve only 0.1% of the volume fraction of atoms in the implanted layer would partition the layer into pieces smaller than 20 nm on average.) In as-implanted samples disordered ion tracks can be easily envisioned as these line defects. On the contrary, it seems that simple point defects, such as interstitials, for example, do not cause enough disturbance in crystal symmetry to directly determine L, so that for such very small defects the effective reduction of L results from cumulative effects on phonon scattering.[30] These effects should be important for very low implantation doses, where implanted ions create disordered cascades that are far apart, and most of the layer is still undamaged. At higher doses, when a considerable part of the layer is disordered, these effects should become irrelevant and changes in volume fractions of perfect and disordered parts of the layer should dominate. Our RS and RBS data give the opportunity to check this concept experimentally and quantitatively, which will be done in the next section.

An important consequence transpires from the above discussion: defects having small volume but different morphology (like clusters of interstitials in contrast to dislocation loops or other linear or planar defects) could influence Raman and RBS spectra very differently. For very small concentrations some of them will be invisible to RBS but can strongly influence Raman spectra by lowering crystal translation symmetry. On the other hand, at large concentrations, where the change of the total disordered volume is the most prominent effect, some of these defects will be sensed by RBS more profoundly than their volume fraction would warrant due to shadowing effects.

B. Dose effects

The measured RS is interpreted as being a superposition of several essentially independent components.[3] In this work we provide arguments that they represent following structures of the implanted layer: undamaged crystalline, recrystallized misoriented crystalline, amorphous CRN, and BP amorphous phase. The essential difference between the present analysis and previous interpretations[4,24,34] is the inclusion of the ''background signal'' as a representative of a new component of the disorder, the second amorphous phase, possibly comprising MRO.

The other important improvement is that, in order to analyze disorder quantitatively and to determine more precisely the bandwidth and position of the LO peak, all other components (including BP) were subtracted in a consistent way: a-BP (''background'') signal approximated with linear function, the a-CRN signal with a Gaussian function, and the TO crystalline peak with a Lorentzian shape function (Fig. 1). The remaining LO peak was then analyzed within the ''spatial correlation'' model[6,37] in which it is assumed that defects introduced by irradiation partition crystal into regions of finite size L. The consequence is the relaxation of the $\mathbf{q}=0$ selection rule, allowing the contributions from $\mathbf{q}\neq 0$ phonons, determined by the dispersion relation $\omega(\mathbf{q})$. The localization of the wave vector is imposed through the Gaussian attenuation function $\exp(-q^2L^2/4)$ and the Raman intensity at a frequency ω is expressed as

$$I(\omega)\sim\int_0^1 \exp\left(\frac{-q^2L^2}{4a^2}\right)\frac{d^3q}{[\omega-\omega(q)]^2+[\Gamma_0/2]^2}, \qquad (1)$$

where $\mathbf{q}$ is the wave vector in the units of $2\pi/a$, a is the lattice constant ($a=5.65$ Å for GaAs crystal), Γ_0 is the full width at half maximum of the unperturbed LO shape and determined from the measurement on undamaged crystal ($\Gamma_0=3.2$ cm^{-1}). For the dispersion relation $\omega(q)$ we have used analytic expression

$$\omega(q)=A+B\cos(\pi q), \qquad (2)$$

which reproduces well the dispersion of the LO phonon in GaAs and has been successfully used by Tiong *et al.*[6] We have chosen slightly different values for parameters in Eq. (2), $A=267.8$ cm^{-1} and $B=22.5$ cm^{-1} to accommodate the fact that our measurements were done at RT instead of at 77 K.[6] The integration is performed numerically and the correlation length L is obtained as a parameter of the fitting curves calculated after Eq. (1) for each dose.

Following implantation, the experimental LO(Γ) line, located at 290 cm^{-1} in the undamaged sample, shifts to lower frequency and broadens asymmetrically (Fig. 1 and inset of Fig. 8). This is the result of the change in the phonon localization length L due to the size reduction of the remaining crystallites[4,6] and possibly due to other factors, such as defect-associated lattice strains.[29] The LO line disappears at the same ion dose and rate in RS for which the fraction of disordered atoms in RBS spectra reaches 100% (Fig. 3).

The peak at 268 cm^{-1} is assigned to the TO phonons. This peak shows a very small redshift and only slight broadening (Fig. 1), in accord with previous reports.[29] We have interpreted it as scattering from parts of the implanted layer that were recrystallized, and misoriented after freezing out of the hot tracks along the ions' path. The arguments for such an interpretation can be deduced from previous papers: (a) the TO peak, although forbidden for (100) orientation, is allowed for different crystal orientations in GaAs,[6,29] and (b) there is no peak or band originating from amorphous phase that could have its maximum at energies higher than 250 cm^{-1} (Refs. 7 and 34). (This work offers further arguments for this assignation); (c) there is a very significant recrystallization of GaAs implanted with Si at RT (considerably lower disorder for RT than for low-T implants; Figs. 6 and 7), and (d) the dose dependence of the relative intensity of the 268-cm^{-1} peak (Fig. 3): its fraction first increases with dose and then decreases down to complete disappearance. This happens for the same dose for which the other crystalline fraction related peak, the LO-phonon peak, disappears as well. The disappearance of both crystalline peaks occurs at lower dose for high dose rate implants, as an expected consequence of rate effects (next paragraph). Additionally, in GaAs implanted at RT, misoriented recrystallized portions of the layer were indeed observed by high-resolution transmission electron microscopy.[38]

The most interesting is the dose dependence of the amorphous-phase related peaks. It is widely accepted that the peak at 250 cm^{-1} originates from the amorphous phase,[3,4,33,34] specifically from the a-CRN structure.[3] The fraction of this component (f_a) increases with ion dose, but only within a limited dose range. For higher doses f_a saturates, and even decreases. On the other hand, the BP fraction f_b increases in the whole range of applied doses (Fig. 3). This result suggests that implanted Si ions, besides destroying crystallinity of the starting material, also change the structure of the amorphous phase. This effect is clearest for the highest doses, when both crystalline fractions are zero, i.e., the implanted layer is completely amorphized. Then a further increase of dose undoubtedly converts the a-CRN fraction into the a-BP fraction. However, it seems that the same effect is occurring at lower doses as well: the stagnation of f_a with dose at intermediate doses can then be explained by postulating simultaneous conversion of crystalline material into amorphous phase(s) along with the conversion of the a-CRN structure into the BP structure, causing first stagnation and then even a decrease of f_a. The evolution of the ratio of both amorphous components I_b/I_a with dose is particularly informative (Fig. 4): at lowest doses, the I_b/I_a ratio remains constant but increases progressively at higher doses.

To obtain a quantitative estimate of the amorphization process with dose increase, we used here the basic approach of the Morehead-Crowder (MC) model.[39] This model attributes damage formation to the quenching-in of a high-density defect cluster within a cylinderlike volume along each ion track. The volume of each such cylinder is equal to $A_{a1}d$, where A_{a1} is the average amorphized single cascade area (projected on the surface of the crystal), and d is penetration depth (i.e., the thickness of the implanted layer). Gibbons[40] has shown that when an allowance is made for those cascades that overlap with preexisting amorphous areas, the effective cumulative amorphized area, $A_{a,\mathrm{eff}}$, covered by cascades in the MC model is

$$A_{a,\mathrm{eff}}=A_{\mathrm{tot}}[1-\exp(-DA_{a1})], \qquad (3)$$

where D stands for the applied dose and A_{tot} for the total implanted area. For doses above a few times 10^{13}/cm^2, the probability for each additional ion cascade to overlap already highly damaged volume becomes significant and increases considerably with dose. Therefore the observed increase of I_b/I_a (Fig. 4) indicates that I_b is more efficiently created indirectly, from already highly predisordered (or even amorphized) material than directly, from the virgin crystal.

Within the fractal interpretation of the BP,[9,10] this structure was discussed in terms of strained nanometric ''blobs''

of host atoms whose overcoordination is relaxed through bond percolation. In that model it was assumed that these blobs are responsible for the ''excess'' vibrational modes and resulting BP. Presented results on dose effects corroborate this picture: Si atoms, being smaller than both Ga and As host atoms, can be envisioned as potential nucleation centers for such strained blobs. Hence higher dose produces more blobs and larger BP. These results and interpretation are also consistent with the results obtained in *a*-Si:H, where addition of C atoms also increases the BP component.[9] At the highest doses the I_b/I_a ratio becomes very large, indicating a tendency toward almost complete ''bosonization'' of the layer. This would mean that the composite of BP and CRN amorphous phases is progressively replaced with a network of strained regions connected through remnants of CRN. Such a picture of disordered solids in which some specific structure with medium range order is connected into a network is currently gaining some favor both in interpretation of experimental results in glassy materials and in theoretical concepts and modeling of these amorphous materials.[41]

The very large I_b/I_a ratio for larger doses gives additional support to the concept of the ''boson peak'' as a manifestation and measure of a new, distinct phase of the disorder, contrasting an alternative model, which attributes the broad peak to the sum of higher-order scattering contributions to the Raman spectrum.[42] Should the latter be the case then, in order to observe such large values of I_b/I_a, one should have to assume that second- and higher-order scattering contributions have similar or even higher intensity than first-order scattering, which would be very hard to justify.

Additional implantation of already amorphized layer brings to the layer both more foreign atoms and more energy, delivered by the impact of accelerated ions. Hence the question is whether the increase of I_b at the expense of I_a results from additional doping (i.e., more nucleation centers) or from the energy delivered to the crystal by the implantation. It remains also unclear which amorphous component, *a*-BP or *a*-CRN configuration, is energetically more favorable and thermally more stable, i.e., whether the energy delivered by fast ions is used to further disorder the layer or to better arrange it into a more favorable configuration. These questions cannot be answered from dose effect experiments alone, but will be discussed more thoroughly when dependence on implant temperature is included in Sec. IV D.

Some additional consequences and conclusions can be obtained by analyzing the evolution of disorder with dose as observed on the same set of samples by RS and RBS (Fig. 3). Even at the lowest dose used the intensity of the LO peaks (Figs. 1 and 3) is considerably reduced. At this low dose (only 0.3% of the CA dose) the volume fraction of all disordered atoms has to be still very low, and RBS measurements confirm that notion. This means that crystal-to-amorphous conversion is not yet important, and hence the primary ''disordering'' mechanism is a decrease of the correlation length L with dose. For higher doses the change of relative volumes of crystalline and amorphous fractions becomes dominant. The considerable change of slope of both I_{LO}/I_a and I_{LO}/I_b ratios with dose at approximately few times $10^{13}/\mathrm{cm}^2$ (Fig. 4) is interpreted as a change from one mechanism into the other.

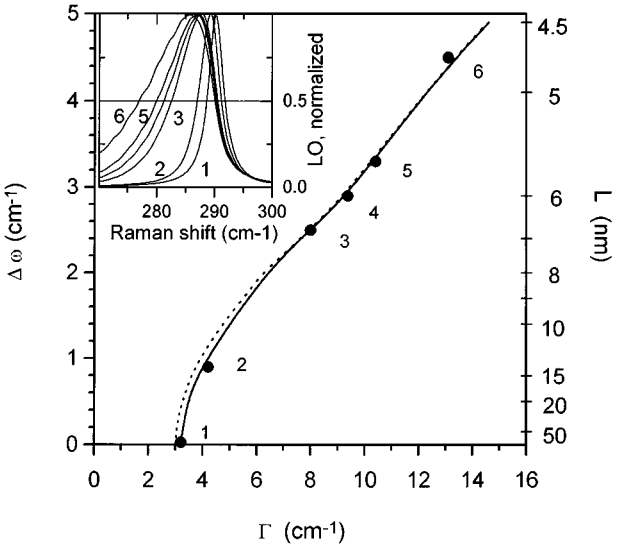

FIG. 8. Calculated Raman shift and line broadening of the LO peak as a function of correlation length L: full line, this work; dashed line, calculated with parameters from Ref. 6. Full circles are experimental values determined from RS spectra after all components except LO were subtracted: (1) unimplanted sample, and 5 different doses: (2) $8\times10^{12}/\mathrm{cm}^2$ (3) $3\times10^{13}/\mathrm{cm}^2$ (4) $2\times10^{14}/\mathrm{cm}^2$, (5) $1\times10^{14}/\mathrm{cm}^2$, and (6) $1\times10^{15}/\mathrm{cm}^2$. Inset: normalized LO peak for same doses.

Fitting parameter L of Eq. (1) allows us to give an independent experimental assessment of the above conclusions. The shift of the LO peak position $\Delta\omega$, calculated from Eq. (1), can be plotted as a function of the LO width Γ as presented in Fig. 8. Right y axis shows corresponding values of L. The full line is calculated from Eq. (1) and the dispersion relation [Eq. (2)] with parameters chosen to account for measurements at RT and used for fitting throughout this work. The dashed line was obtained when Tiong's parameters,[6] appropriate for 77 K, were used. Experimental points were determined from LO peaks obtained from RS spectra for each ion dose, after all other contributions (*a*-CRN, *a*-BP, and TO related RS signals) were subtracted from the deconvoluted measured RS spectra. The agreement between the experimental points and the theoretical curve allows two conclusions. First, that the redshift of LO and its broadening are mainly the consequence of the reduction of L.Therefore other mechanisms (strain, proximity of point defects, etc.[29]), which were not included in Eq. (1), have to be much less important. Second, that the deconvolution process of RS spectra, and hence the underlying physical mechanisms, were correctly chosen.[43]

L values obtained by fitting the LO peak in RS spectra with Eq. (1) (right axes of Fig. 8) are presented as a function of ion dose in Fig. 9 (L_{RS},full circles). L reduces gradually with dose down to 5 nm, or so, and then a sudden change (''quasi-phase transition'') occurs in the implanted layer, with an abrupt transformation from amorphous+crystalline to completely amorphous, where obviously $L=0$. This means that there is no gradual reduction of L down to zero for the CA dose, which one would expect for a smooth and continuous union of neighboring amorphous cascades into a completely amorphized layer. A similar effect was reported

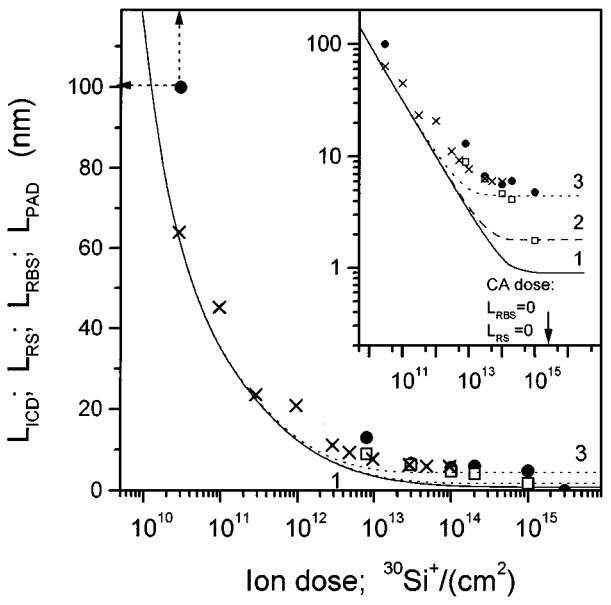

FIG. 9. Dependence of L on ion dose. ●, L_{RS}, values of correlation length determined from RS spectra, [Eq. (1); Fig. 8]; □, L_{RBS} values determined from RBS disordered volume fraction [Eq. (6)]; ×, L_{PAD}, calculated from data in Fig. 3 in Ref. 47, and intercascade distance L_{ICD}, (full line), calculated from Eq. (4), for $D_c = 1.25\times10^{14}$ cm^{-2}. Curve 2 refers to values obtained with $D_c = 4\times10^{13}$ cm^{-2}, and curve 3 with $D_c = 5\times10^{12}$ cm^{-2}. Arrows at the first point indicate that only the lower limit of L can be estimated from Eq. (1), since for larger L fitting becomes insensitive to increase of L, and mechanism(s) limiting L in unimplanted crystal are not known.

for silicon films obtained by glow discharge, where both amorphous and microcrystalline samples were obtained by gradually varying deposition parameters.[44] The absence of a continuous transition was observed, and the crystalline particle size could not be reduced below ~6 nm. Obviously, detailed investigation applying small increment of doses in the range just below the CA dose would provide more information about this exciting subject.

Additionally, we have calculated the average size L_{ICD} of undamaged crystal regions, as a function of ion dose. Following the MC model the partition of the implanted layer reduces to a two-dimensional problem and the average distance between disordered ion cascades L_D can be estimated from $L_D = 1/D^{1/2}$. This relation was also used to estimate the average distance between in-plane point defects in Ar-bombarded graphite.[45] We have modified this model: although it is very reasonable for low doses, it obviously must underestimate L values for higher doses. Namely, when the probability for the overlap of different cascades becomes significant then new cascades become less efficient in partitioning the remaining undamaged parts. Using the same reasoning as for the dose dependence of $A_{a,\mathrm{eff}}$ [Eq. (3)], an effective dose D_{eff} can be defined as $D_{\mathrm{eff}} = D_c[1 - \exp(-D/D_c)]$. D_c denotes some critical dose, which is equal to $1/A_{a1}$, as follows from Eq. (3). Then the effective intercascade distance L_{ICD} can be estimated from

$$L_{ICD} = \frac{1}{\sqrt{D_c[1-\exp(-D/D_c)]}}. \tag{4}$$

Figure 9 shows the calculated L_{ICD} as a function of dose (curve 1). Assuming a reasonable single cascade diameter of 1 nm, $A_{a1} = 8\times10^{-15}$ cm^2 and $D_c = 1.25\times10^{14}$ cm^{-2}. For this value of D_c calculated L_{ICD} are systematically lower than experimentally determined L_{RS} values. However, since both L_{ICD} and L_{RS} were determined without any free, adjustable fitting parameters, we consider the agreement satisfactory. Even better agreement is obtained with somewhat lower D_c values (curves 2 and 3).

A very important conclusion of these considerations and results (presented in Figs. 8 and 9) is that both experimental results (from RS) and theoretical estimates (from intercascade distance model, ICD) show strong reduction of L with dose for lower doses, a notable kink in the 10^{13}–10^{14}-cm^{-2} dose range, and a weaker dose dependence for higher doses. This is in very good agreement with conclusions deduced from the change of slope of LO fraction (Fig. 3) and Raman ratios (Fig. 4), and concept elaborated upon in Sec. IV A. Very close similarity of curves depicting dose dependence of Raman ratios I_{LO}/I_a and I_{LO}/I_b and L_{RS} confirms that Raman ratios in fact measure primarily the reduction of L (and then indirectly through that the increase of damage fraction), particularly at lower doses. The volume transformation of crystalline to amorphous fractions becomes important only at higher doses. Decrease of L_{RS} for higher doses, where calculated L_{ICD} reaches practically a plateau (inset of Fig. 9) reflects the fact that L_{ICD} refers exclusively to effects of partition of crystalline areas, while measured L_{RS} reflects the increase of amorphization with dose as well. Correlation between L_{RS} and L_{ICD} breaks down completely for $D \approx$ CA dose, which is understandable since in Eq. (4) no provision was built in for a sudden transformation of a very highly disordered phase into the completely amorphous phase(s).

A quantitative comparison between RS and RBS is possible through the combination of ICD and MC models that allows us also to estimate L from the RBS experimental data (L_{RBS}). In the MC model the RBS volume damage fraction f_{RBS} corresponds to the fraction of damaged area, so that $f_{RBS} = A_{a,\mathrm{eff}}/A_{\mathrm{tot}}$. Hence, from Eqs. (3) and (4) one obtains

$$L_{RBS} = \frac{1}{\sqrt{D_c f_{RBS}}}. \tag{5}$$

L_{RBS} values presented in Fig. 9 accord reasonably well with L_{ICD} and even better with L_{RS}. Again, note that L_{RBS} was also determined without adjustable parameters. Once again, Eq. (5), for the same reasons as Eq. (4), cannot predict $L_{RBS} = 0$ for the CA dose, which is an obvious value for a completely amorphized layer (Fig. 3). Agreement between L_{ICD}, L_{RB}, and L_{RS} confirms that the concepts of intercascade distance and correlation length, each obtained from very different approaches, assumptions, and approximations, are equivalent. This allows the meaningful comparison of RS and RBS results, but also confirms the validity of the spatial correlation model, which has been often used but also seriously questioned.[29,30]

Unfortunately RBS is insensitive at very low doses, so the comparison with L_{ICD} or L_{RS} in this range is not possible. However, the photoacoustic displacement technique (PAD)

has been recently developed for low dose monitoring.[46] We have used PAD experimental points, which measure the dose dependence of implantation-induced damage in Si-implanted GaAs,[47] and normalized them with RBS data for one dose ($3\times10^{13}/\mathrm{cm}^2$) from the middle of the dose range in which both methods overlap. Dose dependence of L_{PAD} [calculated by a formula analogous with Eq. (5)] shows an excellent agreement with L_{RBS} at other doses, but also with L_{RS}, as well as with L_{ICD} particularly in low dose range. This accord demonstrates that the correlation length concept is the same when measuring the implantation-induced disorder either by RS or RBS or PAD, and that the ICD model describes well L measured by any of these three methods.

An apparently huge difference in sensitivity to disorder at low doses between RBS and RS can now be more directly explained: measure of disorder in RBS (f_{RBS}) reflects the fraction of disordered volume of the disordered layer, while measure(s) of (dis)order in RS (RS ratios or f_{RS}) measure simultaneously two aspects of the disorder: lowering of the translational symmetry (prevailing at low doses) and fraction of disordered volume (effect which prevails at higher doses).

C. Dose rate effects

It has been shown already that the comparison of dose effects and dose rate effects, as observed by RS and RBS could be used to estimate the morphology of dose-rate-induced damage.[25,24] However, since those conclusions were reached without taking into account the ''boson peak'' component, they have to be reassessed. Figure 5 shows the qualitative differences in RBS and RS assessment of the rate-induced disorder. If one takes dose effects (which cover the wide range from almost zero to complete disorder) as a gauge, it is obvious that RBS is very sensitive to rate effects. On the contrary, both I_{LO}/I_a and I_{LO}/I_b ratios are similar and each of them change very little with the change of dose rate. This indicates that the inclusion of the new amorphous component I_b into the physical picture will not change or contradict previous arguments and conclusions.[24,25] In fact, the main result of that analysis, that the rate effects are caused primarily by small volume defects in crystalline phase, has been in the meantime independently endorsed by other methods as well.[48,49] There is separate evidence that these small-volume defects are most likely clusters of interstitial Ga atoms[48] and/or clusters of interstitial As atoms.[49]

An additional conclusion from Fig. 5 is that rate effects cause an increase (although modest) of I_b/I_a ratio, indicating somewhat preferential formation of the BP phase for higher rates. This result is in agreement with trends observed in dose effects, where the increase of total disorder (RBS) is also accompanied with the conversion of I_a into I_b. Therefore, it seems that the BP component is accumulated more easily from already disordered material, independently of whether this disorder is created by dose or rate effects.

For a more quantitative comparison of dose and rate effects the summing of Raman scattering intensities from various phases has to be done. Although neither scattering volumes nor specific scattering cross sections for each phase are known,[50] some crude assessment can be done. We estimated scattering volumes for the extreme situations, corresponding to perfect crystal and to a completely amorphized layer using the penetration depth, $d=1/(2\alpha)$, where α is the absorption coefficient. Taking α for crystalline GaAs from Ref. 51 and for amorphous GaAs from Ref. 52, one obtains that scattering volume for 514.5-nm photons is almost $4\times$ smaller in amorphized GaAs than in the crystal. On the other hand, the total number of photons scattered from a-GaAs is about 30% larger than from c-GaAs. This leads to a weighting factor of about 5 for scattering from an undamaged crystal toward scattering from amorphous phases. Under the assumption that the scattering power of both amorphous components is the same, and, similarly, also the same for both crystalline components, the fraction of RS signal from yet undisordered parts of the implanted layer is $I_{\mathrm{LO}}/[I_{\mathrm{LO}}+I_{\mathrm{TO}}+(I_a+I_b)/5]$. Then the damaged fraction f_{RS} detected by RS for any particular ion dose and rate is

$$f_{\mathrm{RS}}=1-\frac{I_{\mathrm{LO}}}{I_{\mathrm{LO}}+I_{\mathrm{TO}}+(I_a+I_b)/5}, \tag{6}$$

which then can be compared with f_{RBS}, as presented in Fig. 10. Although there is always a correlation between RS and RBS detected disorder, quite different correlations are observed for various dose ranges, depending on whether the ion dose or dose rate is the principal variable. Differences and similarities in the sensitivity of each method to specific types of defects (disorder) are now very clear. At low doses, where the total number of displaced atoms is very small (and hence f_{RBS} is very small), the extended defects formed along the ion tracks cause a strong increase of Raman damage fraction (due to the decrease of the L). On the contrary, RBS is much more sensitive to the increase of concentration of dose-rate-induced defects, which—although small in volume—still obstruct a large fraction of the open channels for the RBS probing beam. However, both methods are comparably sensitive when monitoring the increase of the volume of disordered

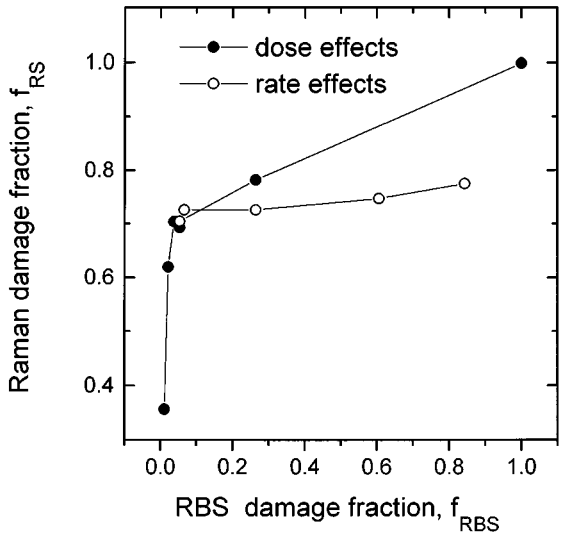

FIG. 10. Correlation between Raman detected disorder and RBS detected disorder for different ion doses (solid symbols) and dose rates (open symbols). Normalized Raman detected disorder is defined as $f_{\mathrm{RS}}=1-I_{\mathrm{LO}}/[I_{\mathrm{LO}}+I_{\mathrm{TO}}+(I_a+I_b)/5]$, in accord with Eq. (6). Lines are added to guide the eye.

fractions (primarily f_a and f_b; Fig. 3) at the expense of undamaged crystal. Hence, the results show that several different types of disorder could be recognized and separated by comparative study of RBS and RS.

D. Implant temperature effects

RBS measurements on Si-implanted GaAs demonstrated a very strong dependence of the total amount of disorder on the temperature at which the implantation was performed.[25,53] The disorder decreases systematically as the implant temperature is increased in the temperature range around RT. The decrease is especially sharp for high doses. These measurements give direct evidence for significant dynamic annealing (self-healing) in GaAs; i.e., a large fraction of the implantation-induced disorder is removed during the implantation process itself.

Comparative study with RS provides additional information about effects involved in these drastic changes (Figs. 6 and 7). The disorder detected by RS shows the same trends as RBS, both considering different doses at some selected temperature, or considering different implant temperature for a selected dose: the RS measure of crystal perfection (I_{LO}/I_a or I_{LO}/I_b ratios) show improvement of crystallinity for lower doses and higher implant temperatures. However, again there are considerable quantitative differences in how sensitive two methods are to the disorder. The difference at the high damage end (low implant temperatures) is probably less informative. Nonzero RS ratios (reflecting the existence of small LO fraction) are most probably caused by the remnants of some crystallites close to the surface in the nearly amorphized layer. The more important quantitative difference is at the low-damage end, where I_{LO}/I_a and I_{LO}/I_b ratios are far from being as high as one would expect for the GaAs crystal in which RBS detects almost no damage. Obviously, I_{LO} is much too small for the supposedly almost undamaged crystal. In accordance with discussion in Secs. IV A–IV C, one has to conclude that there must exist an abundance of specific types of residual defects, which lowers the LO fraction. Since f_{RBS} is very low, these defects are most likely of the same types as defects that lower the LO fraction at very low implant doses, i.e., small-volume but elongated (linear, planar, extended, etc.) defects. This conclusion is in agreement with findings obtained with other methods, which showed that implanted and annealed GaAs contains considerable concentration of dislocations loops, stacking faults and other extended defects,[25] planar defects, etc.[38] It is interesting that the I_{LO}/I_a and I_{LO}/I_b ratios remain constant above some implant temperature, indicating some residual disorder that is temperature resistant in this temperature range (Fig. 6). Some of these defects survive even high-temperature annealing, causing problems in electrical activation of dopants.[25] Lower ratios for higher implantation doses at any implantation temperature indicate that the concentration of these residual line/planar defects is positively correlated with dose.

Another interesting question is whether the drastic reduction of total disorder for high-T implants, as observed by RBS, reflects a proportional reduction of all components of the disorder. The MC model[39] describes fairly well the temperature dependence of total damage,[53] and predicts that there will be a critical temperature, independent of ion dose, at which the direct-impact damage vanishes. It is very interesting that, for a wide range of ion doses, the change of the morphology of the amorphous volume (evaluated by change of I_b/I_a ratio) follows exactly the same trend as total damage (Fig. 7) and its prediction by the MC model.[53] This indicates that the BP structure is more vulnerable to thermally activated diffusion of atoms from the cascades. RBS results show that total disordered volume (and probably volume of each cascade as well) is up to 2 orders of magnitude smaller if the implantation is done at 40 °C instead of RT. The BP fraction is reduced even 2 times more. Hence the BP component is thermally less stable than the a-CRN component of the disorder, which means that the free energy of the CRN structure is lower than the free energy of the BP structure.

At lower implant temperatures, the total disorder is larger because a larger part of each cascade remains highly disordered, effectively increasing the probability of the overlap of different cascades. The observed strong increase of I_b/I_a indicates more efficient production, growth, and accumulation, of the BP structure for conditions where implanted ions enter into the already disordered crystal. The same result is observed in dose effects (Fig. 4) and rate effects (Fig. 5) as well. Hence, independently of the type of the disorder and how it is produced, the a-BP structure is formed preferentially over the a-CRN component from predisordered GaAs, rather than directly from the crystal. This seems to be a universal and important property of a-BP.

Furthermore, the I_b/I_a ratio at any temperature (within applied range) is higher for larger ion dose, consistent with the interpretation that BP originates from strained bonds between small Si atom and host atoms (Sec. IV B). However, BP is not caused by the presence of foreign atoms only, since for the same dose (i.e., the same concentration of Si atoms) the relative BP intensity as well as the I_b/I_a ratio vary considerably with implant temperature as well as with dose rate. It seems that the increase of total disorder (Figs. 5 and 7) and the resulting increase of strain between differently disordered parts of the layer is sufficient to increase the BP component. Consequently, all experimental results regarding the BP component can be interpreted consistently by postulating that strained bonds both inside strained blobs and at their boundaries (interfaces with the relaxed surrounding) cause ''excess'' vibrational states that are manifest as the BP component of the disorder in Raman spectra. Within this picture both implant temperature dependence, rate, and dose dependence of growth and accumulation of different phases of the disorder can be explained consistently.

The ability to create the BP structure in a controlled way by ion implantation is unique and important, offering a number of exciting possibilities in future experiments. They should lead to a better understanding of a-BP in tetrahedrally coordinated semiconductors. It also raises confidence in the solution of this long-standing problem in glasses as well, where BP structure is inherently present, hence it cannot be either created or annihilated controllably.

V. CONCLUSIONS

GaAs crystals were implanted in a wide range of ion doses, ion-dose rates, and implant temperatures and analyzed

with Raman scattering (RS) and ion channeling (RBS). RS spectra were deconvoluted consistently and systematically into up to four components, one of them being apparent background signal interpreted here as a boson peak. Arguments are given that this signal represents the second amorphous phase different from *a*-CRN.

We have postulated an intercascade distance model (ICD) that estimates the average distance L_{ICD} between implantation-induced cascades as a function of ion dose. An analogous parameter L_{RBS} was calculated from RBS data for damage fraction f_{RBS}. From RS data the correlation length L_{RS}, representing the size of crystalline regions over which the order and translational symmetry is preserved, was determined by fitting of LO signal within the SC model. All three L's (as well as L_{PAD} obtained from PAD data for low doses) agree nicely, proving that the correlation length in RS and intercascade distance in RBS are equivalent. This enabled a straightforward comparison of relevant signals and a direct correlation between RS and RBS determined disorder. While measure of disorder in RBS (f_{RBS}) reflects the disordered volume fraction of the implanted layer, RS measures simultaneously lowering of the translational symmetry (an effect that prevails at lower doses) and fraction of disordered volume (prevailing at higher doses). Still f_{RBS} and f_{RS} remain directly proportional even at low doses since there $f_{\mathrm{RS}} \approx L^{-2}$ while $L \approx D^{-(1/2)}$. Considerable differences in sensitivity to particular defects were used to differentiate damage. Six different types of implantation-introduced disorder were successfully resolved.

ACKNOWLEDGMENTS

This research was supported by the Ministry of Science and Technology of Croatia. A portion of this research was performed at Oak Ridge National Laboratory, sponsored by U.S. Department of Energy, Division of Materials Science, under Contract No. DE-AC05-960R22464 with Lockheed Martin Energy Research Corp.

[1] S. J. Pearton, F. Ren, S. N. G. Chu, W. S. Hobson, C. R. Abernathy, T. R. Fullowan, J. R. Lothian, R. G. Elliman, D. C. Jacobson, and J. M. Poate, Nucl. Instrum. Methods B **79**, 648 (1993); N. Tzenov, M. Tzolov, D. Dimova-Malinovska, T. Tsvetkova, C. Angelov, G. Andriaenssens, and H. Pattyn, *ibid*. **84**, 195 (1994).

[2] S. Roorda, W. C. Sinke, J. M. Poate, D. C. Jacobson, S. Dierker, B. S. Dennis, D. J. Eaglesham, F. Spaepen, and P. Fuos, Phys. Rev. B **44**, 3702 (1991), and references therein.

[3] R. Zallen, J. Non-Cryst. Solids **141**, 227 (1992); and R. Zallen, *The Physics of Amorphous Solids* (Wiley, New York, 1983).

[4] M. Holtz, R. Zallen, O. Brafman, and S. Matteson, Phys. Rev. B **37**, 4609 (1988).

[5] R. Ares, Y. B. Trudeau, J. L. Brebner, G. E. Kajrys, and M. Jouanne, Nucl. Instrum. Methods B **90**, 419 (1994).

[6] K. K. Tiong, P. M. Amirtharaj, F. H. Pollak, and D. E. Aspnes, Appl. Phys. Lett. **44**, 122 (1984).

[7] T. Nakamura and T. Katoda, J. Appl. Phys. **53**, 5870 (1982).

[8] M. Ivanda, Phys. Rev. B **46**, 14 893 (1992).

[9] M. Ivanda, I. Hartman, and W. Kiefer, Phys. Rev. B **51**, 1567 (1995).

[10] M. Ivanda, U. V. Desnica, and T. E. Haynes, Mater. Sci. Forum **143-147**, 1387 (1994); U. V. Desnica, I. D. Desnica, M. Ivanda, and T. E. Haynes, Nucl. Instrum. Methods B **120**, 236 (1996).

[11] Up to now ''boson peak'' has been reported in *a*-Si:H (Ref. 8) and *a*-$Si_{1-x}C_x$:H (Ref. 9); also in *a*-Si [O. Gamulin, M. Ivanda, and U. Desnica, J. Mol. Struct. (to be published)]. Furthermore, there are indications that BP exists in other tetrahedrally coordinated semiconductors, but has not been recognized as such, particularly in Si [Fig. 1 in K. P. Jain, A. K. Shukla, R. Ashokan, S. C. Abbi, and M. Balkanski, Phys. Rev. B **32**, 6688 (1985)]; in Ge [Fig. 1 in J. S. Lannin, J. Non-Cryst. Solids **141**, 233 (1992)]; in AlSb [Fig. 4 in S. G. Kim, H. Asahi, M. Seta, S. Emura, H. Watanabe, S. Gonda, and H. Tanoue, J. Appl. Phys. **74**, 2300 (1993)], etc.

[12] S. Hunklinger and A. K. Raychaunary, in *Progress in Low-Temperature Physics*, Vol. 9, edited by D. F. Brewer (North-Holland, Amsterdam, 1986), p. 205.

[13] V. K. Malinovski and A. P. Sokolov, Solid State Commun. **57**, 759 (1986).

[14] J. Jäckle, in *Amorphous Solids, Low-Temperature Properties*, edited by W. A. Philips (Springer, Berlin, 1981), p. 135.

[15] T. Ohsaka and T. Ihara, Phys. Rev. B **50**, 9569 (1994).

[16] E. Duval, A. Boukenter, and T. Achibat, J. Phys. Condens. Matter **2**, 10 227 (1990).

[17] U. Buchenan, Yu. M. Galperin, V. L. Gurevich, and H. R. Schober, Phys. Rev. B **43**, 5039 (1991).

[18] C. C. Yu, Phys. Rev. Lett. **63**, 1160 (1989); S. N. Coppersmith, *ibid*. **67**, 2315 (1991).

[19] J. E. Graebner, B. Golding, and L. C. Allen, Phys. Rev. B **34**, 5696 (1986); C. Yu and J. J. Freeman, *ibid*. **36**, 7620 (1987).

[20] R. Orbach, Science **231**, 814 (1986).

[21] A. J. Scholten and J. I. Dijkhuis, Phys. Rev. B **53**, 3837 (1996).

[22] R. S. Elliott, Adv. Phys. **38**, 1-88 (1989); Europhys. Lett. **19**, 201 (1992).

[23] R. Roy, Science **238**, 1664 (1987).

[24] U. V. Desnica, J. Wagner, T. E. Haynes, and O. W. Holland, J. Appl. Phys. **71**, 2591 (1992).

[25] T. E. Haynes, O. W. Holland, and U. V. Desnica, in *Advanced III-V Compound Semiconductor Growth, Processing and Devices*, edited by S. J. Pearton, D. K. Sadana, and J. M. Zavada, MRS Symposia Proceedings No. 240 (Materials Research Society, Pittsburgh, 1992), pp. 823–827.

[26] J. C. Bourgoin, J. F. Morhange, and R. Beserman, Radiat. Eff. **22**, 205 (1974).

[27] T. E. Haynes, R. Morton, and S. S. Lau, in *III-V Electronic and Photonic Device Fabrication and Performance*, edited by K. S. Jones, H. Kanber, and S. J. Pearton, MRS Symposia Proceedings No. 300 (Materials Research Society, Pittsburgh, PA, 1993), p. 311.

[28] T. E. Haynes, R. Morton, and S. S. Lau, Appl. Phys. Lett. **64**, 991 (1944).

[29] G. Burns, F. H. Dacol, C. R. Wie, E. Burnstein, and M. Cardona, Solid State Commun. **62**, 449 (1987).

[30] G. Braunstein, D. Tuschel, S. Chen, and S.-T. Lee, J. Appl. Phys. **66**, 3515 (1989).

[31] F. H. Eisen, in *Channeling*, edited by D. V. Morgan (Wiley, New York, 1973), pp. 417–419.
[32] G. Carter, M. J. Nobes, and S. Tashlykov, Radiat. Eff. Lett. **85**, 37 (1984).
[33] The band at 250 $cm^{-1}$is interpreted regularly as TO mode of the amorphous phase. It has been argued recently that this broad band is, in fact, a superposition of two amorphous bands, LO at 220 cm^{-1} and TO at 260 cm^{-1} [M. Ivanda, U. V. Desnica, T. Haynes, H. Hartman, and W. Kiefer, J. Mol. Struct. **348**, 33 (1995)]. As this question is of no importance for this work, we shall retain here the traditional assignment for this mode as being a single mode.
[34] J. Wagner and C. R. Fritzsche, J. Appl. Phys. **64**, 808 (1988).
[35] H. G. Robinson, T. E. Haynes, E. L. Allen, C. C. Lee, M. D. Deal, and K. S. Jones, J. Appl. Phys. **76**, 4571 (1994).
[36] K. Ishioka, K. G. Nakamura, and M. Kitajama, Phys. Rev. B **52**, 2539 (1995).
[37] H. Richter, Z. P. Wang, and L. Ley, Solid State Commun. **39**, 625 (1981).
[38] B. A. Turkot, D. V. Forbes, J. J. Coleman, L. E. Rehn, M. A. Kirk, and P. M. Baldo, J. Appl. Phys. **78**, 97 (1995).
[39] F. F. Morehead and L. Crowder, Radiat. Eff. **6**, 27 (1970).
[40] J. F. Gibbons, Proc. IEEE **60**, 1062 (1972).
[41] J. Non-Cryst. Solids **192&193** (1995), special issue on Structure of Non-Crystalline Materials 6, edited by L. Červinka and A. C. Wright; see in particular H. P. Gaskell, pp. 9–22, and L. W. Hobbs, pp. 79–91.
[42] A. Chehaidar, A. Zwick, R. Carles, and J. Bandet, Phys. Rev. B **50**, 5345 (1994); A. Zwick and R. Carles, *ibid*. **48**, 6024 (1993).
[43] This second point can be traced as a main culprit in Ref. 6 for the systematic shift of experimental data from the theoretical curve given by Eq. (1): one can reconstruct from Fig. 2 in Ref. 6 that the ''experimental'' FWHM was determined from the experimental spectra after subtracting ''background,'' as an arbitrary chosen constant, and without taking into account TO peak. This makes LO peak to appear broader than it actually is.
[44] R. Tsu, S. S. Chao, M. Izu, S. R. Ovshinsky, G. J. Jan, and F. H. Pollak, J. Phys. (Paris) Colloq. **42**, C4-269 (1981).
[45] K. Nakamura and M. Kitajima, Phys. Rev. B **45**, 78 (1992); **45**, 5678 (1992); E. Asari, I. Kamioka, K. G. Nakamura, T. Kawabe, W. A. Lewis, and M. Kitajima, *ibid*. **49**, 1011 (1994).
[46] H. Takamatsu, Y. Nishimoto, and Y. Nakai, Jpn. J. Appl. Phys. **29**, L1025 (1990).
[47] T. Hara, T. Muraki, S. Takeda, N. Uchitomi, Y. Kitaura, and G. Gao, Jpn. J. Appl. Phys. **33**, L1435 (1994).
[48] P. Ehrhart, K. Karsten, and A. Pillukat, in *Beam-Solid Interactions: Fundamentals and Applications*, edited by M. A. Nastasi *et al.*, MRS Symposia Proceedings No. 279 (Materials Research Society, Pittsburgh, 1993), p. 579.
[49] D. Stievenard, X. Boddaert, J. C. Bourgoin, and H. J. von Bardeleben, Phys. Rev. B **41**, 5271 (1990).
[50] The apparently large fractions of disordered components that appear in RS already at the lowest doses, being also much larger than the RBS disorder fraction would suggest that cross sections for disordered components are considerably higher than the cross section for undisturbed crystal. Although there is no reason to expect the same value of the cross sections, such a large difference is puzzling. Comparison to the much more extensively studied amorphous/crystalline silicon is also not very helpful, since reported cross sections for this material are quite contradictory, ranging from higher cross section for the amorphous phase [A. T. Voutsas, M. K. Hatalis, J. Boyce, and A. Chiang, J. Appl. Phys. **78**, 6999 (1995); H. Kanimuna, M. Mohri, M. Sakmoto, and T. Tsurokoka, *ibid.* **70**, 7374 (1991)] to equal values for both phases [C. Godet, B. Marchon, and M. P. Schmidt, Thin Solid Films **155**, 227 (1987)] up to higher value for crystalline phase [A. B. Pevtsov, V. Yu. Davydov, N. A. Feoktistov, and V. G. Karpov, Phys. Rev. B **52**, 995 (1995)].
[51] D. E. Aspens and A. A. Studna, Phys. Rev. B **27**, 985 (1983).
[52] J. B. Theeten and P. Chombon, J. Vac. Sci. Technol. **20**, 471 (1982).
[53] T. E. Haynes and O. W. Holland, Appl. Phys. Lett. **59**, 452 (1991).